

Optical properties of ZnI₂ films

Pankaj Tyagi and A. G. Vedeshwar*

Thin Film Laboratory, Department of Physics and Astrophysics, University of Delhi, Delhi, 110 007, India

(Received 10 April 2001; revised manuscript received 19 July 2001; published 28 November 2001)

The optical-absorption measurements are reported for ZnI₂ films. The optical band gap of stoichiometric, tetragonally structured ZnI₂ films found to be of direct type. The thickness dependence of band gap is attributed to the compressive residual stress in the film. The variation of residual stress with film thickness correlates well with the thickness dependence of packing density and size distribution of crystallite grains as observed by morphological analysis. Band gap was found to decrease with residual stress linearly yielding a band gap of 4.75 eV for a stress-free perfect crystal. The absorption data reveal an excitonic absorption peak at 3.5 eV with a binding energy of 660 meV at room temperature.

DOI: 10.1103/PhysRevB.64.245406

PACS number(s): 81.15.Ef, 78.40.Fy, 78.66.Li

I. INTRODUCTION

The materials having layered structure have been interesting due to their unique physical properties, especially the electronic structure. Mainly, the chalcogenide and halide compounds exhibit layered structure¹ that consists of a strong covalent bond within the layer and a weak van der Waal bond between layers stacked along the third direction. This arrangement could lead to structural polytypes, energy-band anisotropy, exciton state, etc. With exception of structural² and thermochemical³ studies, ZnI₂, unlike other group IIb iodides, has not been extensively investigated. For example, another member CdI₂ has been extensively studied due to its polytypism, while HgI₂ has also been studied to some extent regarding its optical properties and theoretical band structure due to its utility as radiation detector. We have also studied them in thin-film form^{4,5} and extended such studies to ZnI₂. Therefore, we report here our systematic study on structural and optical properties of ZnI₂ films.

II. EXPERIMENTAL DETAILS

Thin films of ZnI₂ were grown on glass substrates (2 cm × 6 cm) at room temperature by thermal evaporation using a molybdenum boat. The starting material was a high-purity analar-grade stoichiometric powder, which was pelletized for evaporation. All the films used in this study were grown at the vacuum of 10⁻⁶ Torr. The deposition rate was optimized at 1–2 nm/s to grow uniform good quality films. Since ZnI₂ is highly hygroscopic the film growth and measurements were carried out under low relative humidity (~40%) condition. However, films observed to be deteriorating only at relative humidity more than 65%. The film thickness was monitored during the growth by a quartz-crystal thickness monitor and was subsequently confirmed by a mechanical stylus method (Dektak IIA surface profiler). The structural studies of the films were carried out by x-ray diffraction (PHILLIPS X-Pert model - 1830). The morphology and chemical composition of the films were studied by scanning electron microscope (SEM) and energy dispersive x-ray analysis (EDAX) (JEOL - 840). The optical-absorption measurements were carried out using a ultraviolet/visible spectrophotometer (Shimadzu UV-260). Small pieces (1

× 1 cm²) of the same film were used for various analyses.

III. RESULTS AND DISCUSSIONS

All the films grown at room temperature were translucent, stoichiometric, and polycrystalline without any exception. The x-ray-diffraction analysis reveals the tetragonal structure of ZnI₂ films with cell parameters $a=0.434$ nm and $c=1.18$ nm ($c/a=2.72$) agreeing very well with powder data ASTM card No. 10–72 and the earlier report.⁶ However, another earlier report² on structural data as well as ASTM No. 30–1479 show $a=1.2284$ nm and $c=2.3582$ nm ($c/a=1.92$). There are three major peaks (101), (102), and (104) in the diffractogram as shown in Fig. 1. The relative intensities of these three peaks vary with film thickness. However, the change in their relative intensities does not reflect any correlation with other parameters like optical properties. Since the peaks in the diffractogram represent the crystal planes parallel to substrate plane and the planes (101), (102), and (104) are all nonparallel planes with different angles to the basal plane of the unit cell, we can realize a random orientation of crystallites that can also be observed in morphology. There are few more smaller peaks of the reflections from (201), (202), (204), and (107) in the diffractogram. The x-ray diffraction data show a small change in the d -spacing of the diffraction peaks. A small deviation in d -spacing could be due to the residual tensile or compressive strain in the film that is quite common in thin films. Thus, the maximum strain determined by $\Delta d/d$ can be multiplied by the elastic modulus to give the maximum stress present in the film. However, no such data is available for ZnI₂. If the fractional change in d spacing given by $\Delta d/d$ compares with line broadening $\Delta(2\theta)$ by the relation,^{7,8}

$$\frac{\Delta d}{d} = \frac{\Delta(2\theta)}{2 \tan \theta}, \quad (1)$$

then we can attribute the change to the residual stress. In the present study, $\Delta d/d$ correlates well with $\Delta(2\theta)$ by relation (1) showing the residual stress in the film. However, line broadening $\Delta(2\theta)$ can also be due to diminishing particle size. If it is due to particle size, the observed $\Delta(2\theta)$ corresponds to 20–80 nm particle size. We have observed mini-

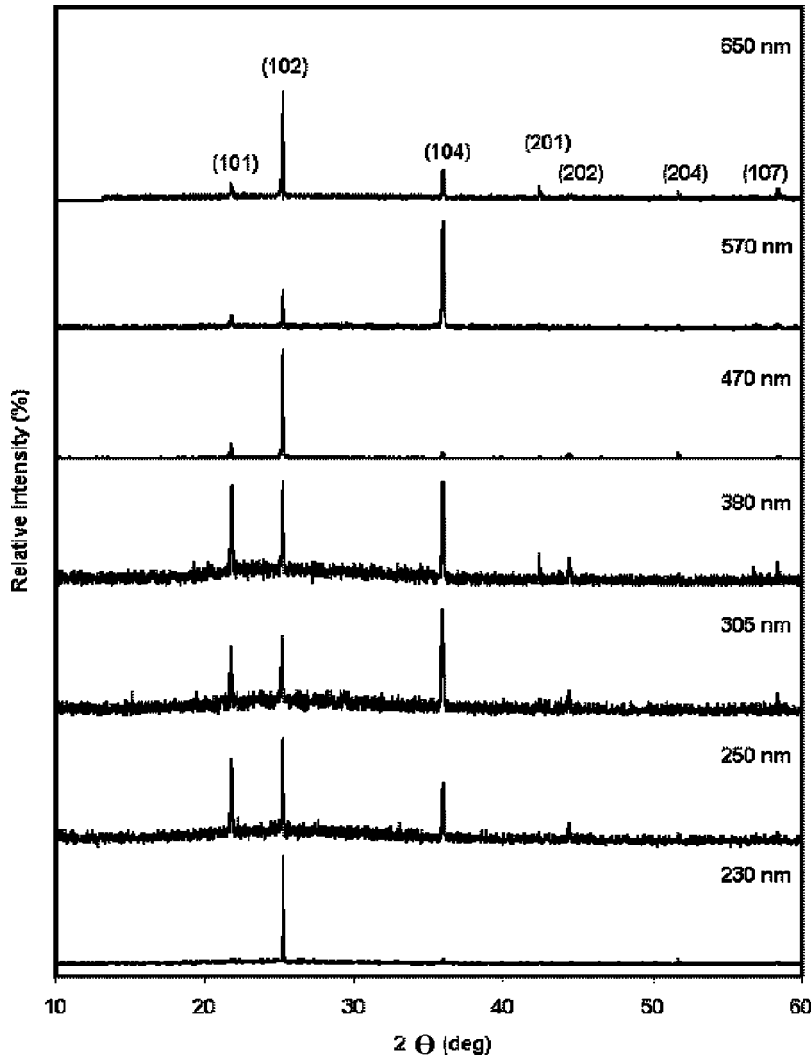


FIG. 1. The x-ray diffraction pattern of ZnI_2 films of different thickness (indicated at each pattern).

imum particle size bigger than 400 nm from SEM analysis. Therefore, we can rule out the contribution of particle size in the present case.

The residual stress could be minimum and uniform in case of crystallites-oriented films. In case of random crystallite orientations, the residual stress on different crystal planes could be nonuniform and different both magnitude and direction wise. It can easily be realized in such cases that the compressive stress on some planes would result in a tensile stress on their orthogonal planes. We have calculated

$$\frac{\Delta d}{d} = \frac{d_{hkl}(ASTM) - d_{hkl}(Observed)}{d_{hkl}(ASTM)} \quad (2)$$

for all possible peaks in the diffractogram. Except (201) all the planes show positive value of $\Delta d/d$ of different magnitudes revealing a compressive stress. However, (201) shows initially very small tensile stress for two-film thicknesses and then switches to compressive stress. The nonuniform stress of different magnitudes on different planes is observed to be in the same direction (i.e., compressive) and show the same trend with film thickness. This could be due to all nonorthogonal and similar planes observed in the diffractogram. Since the magnitude of compressive stress is different for

different planes, we have taken the average of all the planes excluding the negligible tensile stress of (201) for initial two-film thicknesses. The residual-stress parameter $\Delta d/d$ varies with film thickness as shown in Fig. 2. The residual stress increases with film thickness initially and then saturates. This kind of behavior has been observed in thermally evaporated ZnS and CdTe films on silica substrates.⁹ In Ref. 9 the internal stress has been measured by interferometric method. In the same report MgF_2 and CeF_3 films also show similar behavior except a slight decrease after saturation. However, there is not much explanation regarding this behavior. In fact, it is quite difficult to summarize the various stress data on evaporated films into a neat picture because it depends on growth conditions like choice of substrate, substrate temperature, deposition rate, vacuum level, etc. Compressive stresses are observed in many evaporated films.⁸ The compressive stress has also been observed in gas-absorbing films. It should be noted that ZnI_2 is highly hygroscopic and could absorb a very small amount of water vapor when exposed to air in spite of our special arrangements of measurements. Even though, there have been many models in the literature⁸ to explain the internal stress behavior, one of the models, the density effect or packing density of film seems to be appro-

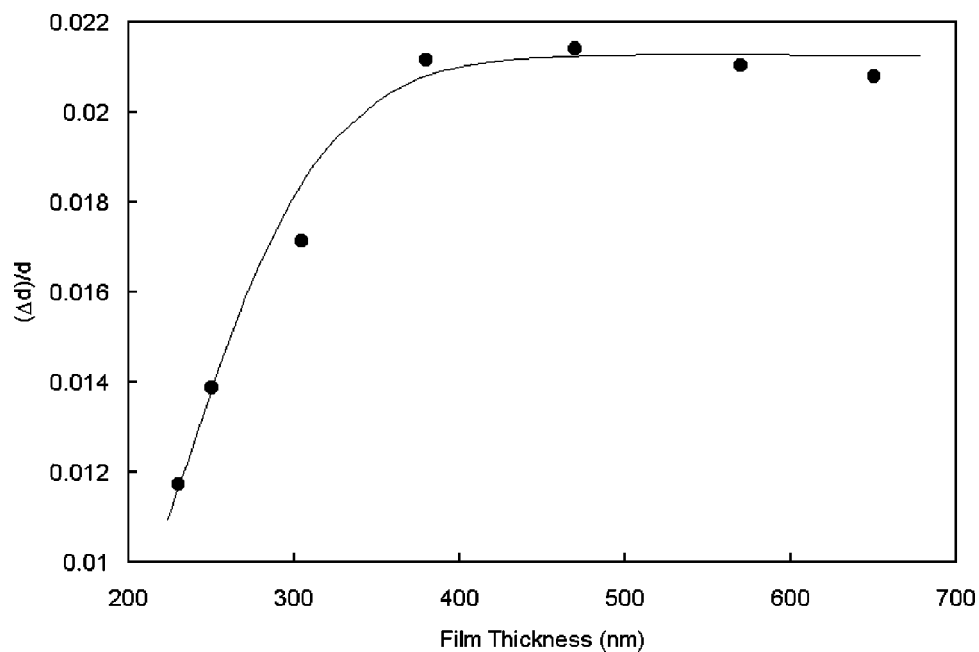


FIG. 2. The residual-stress parameter $\Delta d/d$ as a function of ZnI₂ film thickness.

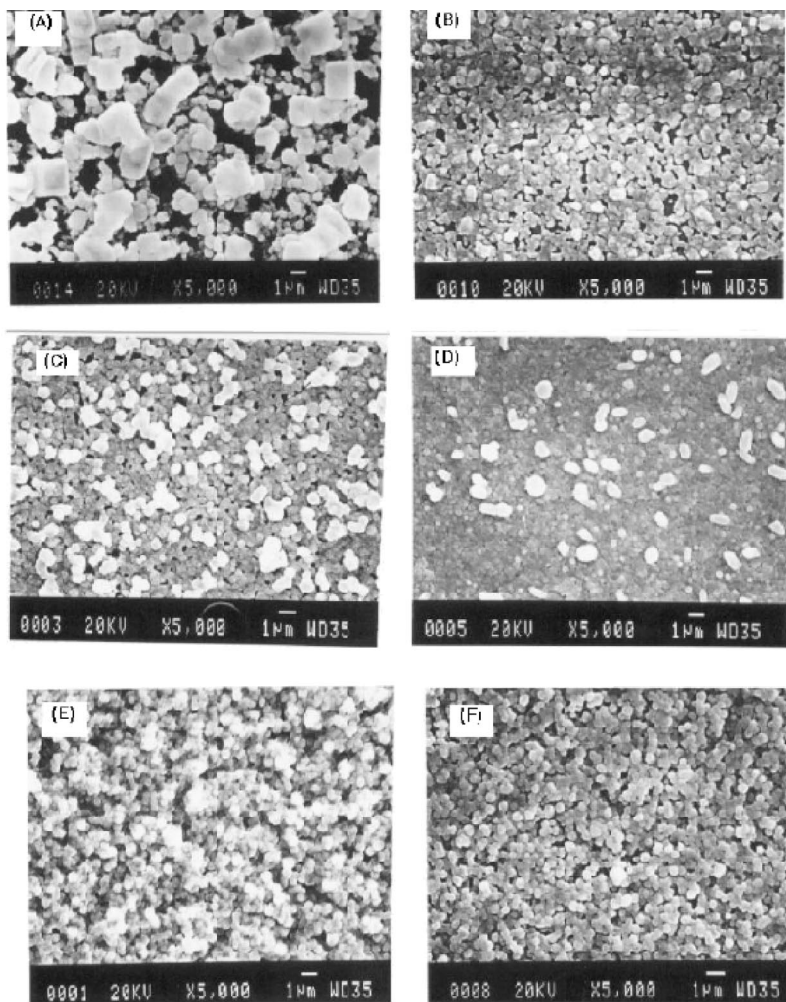


FIG. 3. SEM photographs depicting the crystallite grain morphology of ZnI₂ films of various thickness (A) 230 nm, (B) 250 nm, (C) 305 nm, (D) 350 nm, (E) 570 nm, and (F) 650 nm.

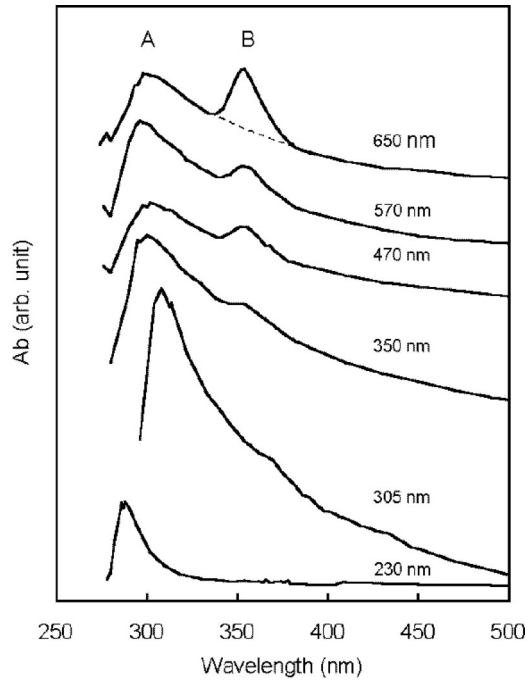


FIG. 4. The optical-absorption spectra for ZnI_2 films of various thickness (identified in the figure). Small peak at *B* is excitonic absorption and *A* is the corresponding interband transition.

appropriate to explain the present behavior. The packing density and grain size distribution improves with film thickness as shown by SEM in Fig. 3. We strongly believe that the observed stress behavior with film thickness is qualitatively due to the packing density of the film and is consistent with SEM results.

The optical absorption as a function of incident photon wavelength is shown for different film thickness in Fig. 4. The absorption curves shown in the figure represent interband absorption region. We can see the development of a small structure at position *B* marked in the figure with increasing film thickness. We speculate it to be excitonic absorption even at room temperature, which is quite possible in case of halides. The excitonic peak that is quite prominent

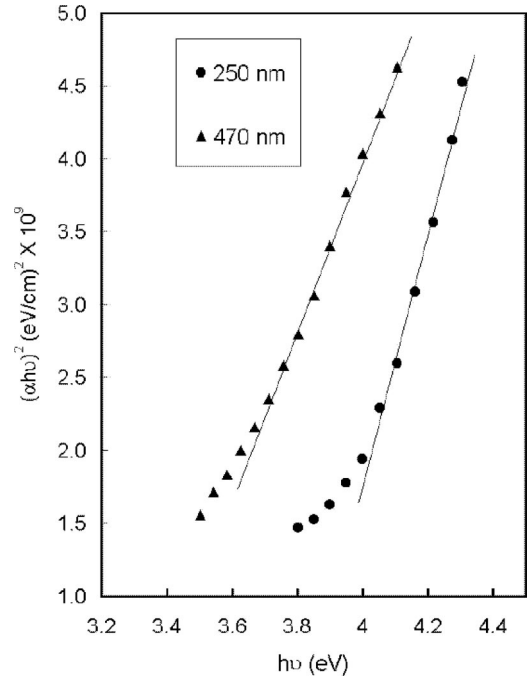


FIG. 5. $(\alpha h\nu)^2$ vs $h\nu$ plot for ZnI_2 films of two different thickness showing the direct type of transition across the band gap.

for thickest film is observed at 3.5 eV. If we assign the peak at *A* (4.16 eV) as due to the associated interband edge concerning the exciton, we get the binding energy of the exciton to be 660 meV. This seems to be quite consistent as compared to few other halides like KI(480 meV), KCl,KBr(400 meV), RbCl(440 meV), and LiF(1000 meV) (Ref. 10). However, a better understanding of the excitonic absorption may be possible by low-temperature measurements. It can be treated only as of indicative nature in the present case.

A routine analysis can be carried out using the absorption curves to determine the magnitude and nature of optical band gap of ZnI_2 . The nature of the band gap, direct or indirect type can be determined by plotting $(\alpha h\nu)^{1/n}$ vs $h\nu$ plot. The exponent $n=1/2$ or $3/2$ for allowed or forbidden direct transition and $n=2$ or 3 for allowed or forbidden indirect type of

TABLE I. Comparison of some structural and optical data of group II*b* iodides.

Material	<i>a</i> (nm)	<i>c</i> (nm)	<i>c/a</i>	E_g (eV)	Ref.
ZnI_2 (Tetragonal)	0.434	1.18	2.72	4.05 (Direct)	Present work, Ref. 6 Ref. 2
	1.2284	2.3582	1.92		
CdI_2 (Hexagonal) (Polytype)					
2H	0.418	0.6736	1.611	3.8 (Direct) 3.2 (Indirect)	Ref. 12
4H	0.418	1.3472	3.22	Same	Refs. 4,13
HgI_2 (Tetragonal)	0.436	1.245	2.86	2.13 (Direct)	Refs. 5,14 Ref. 15
				(Anisotropic)	
(Orthorhombic)				2.55 (Direct)	Ref. 16

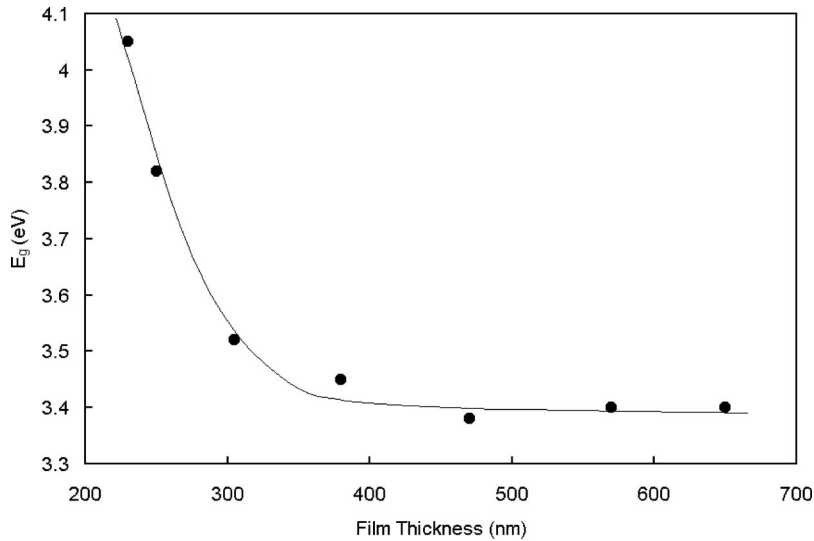


FIG. 6. Thickness dependence of optical band gap for ZnI₂ films.

transition.¹¹ The direct transition gives a single linear portion and its extrapolation yields the direct band gap. The indirect transition yields two linear portions giving rise to two extrapolations ($E_g + E_p$) and ($E_g - E_p$), where E_p is the phonon energy assisting the transition. The absorption coefficient α as a function of incident photon energy $h\nu$ can be calculated using the relation

$$\alpha = \frac{2.303A}{d}, \quad (3)$$

where d is film thickness, by the absorbance curves of Fig. 4. We neglect the excitonic peak and draw a smooth curve (broken line) as shown in the uppermost spectrum for the calculation of α as a function of $h\nu$. We have tried all the exponents and the best fit was obtained for $n=1/2$ to the

measured absorption data as shown in Fig. 5 for only two-film thickness for the purpose of clarity. This shows the nature of band gap as direct type for ZnI₂. We have compared some structural and optical properties of group IIb iodides in Table I.

There is no information regarding band gap of ZnI₂ except the present paper. All three compounds exhibit layered structure and CdI₂ is a well-known polytype material. However, the optical band gap has been found to be insensitive to polytypism or c/a ratio as shown in the table. There are few band-structure calculations for CdI₂ mostly predicting both direct and indirect gaps confirming some experimental results. More details can be found in Ref. 4. HgI₂ is also studied both experimentally and theoretically regarding its band structure. Few experiments have revealed its anisotropic nature of optical properties, that is, parallel and perpendicular to c axis. We have given the common values of the param-

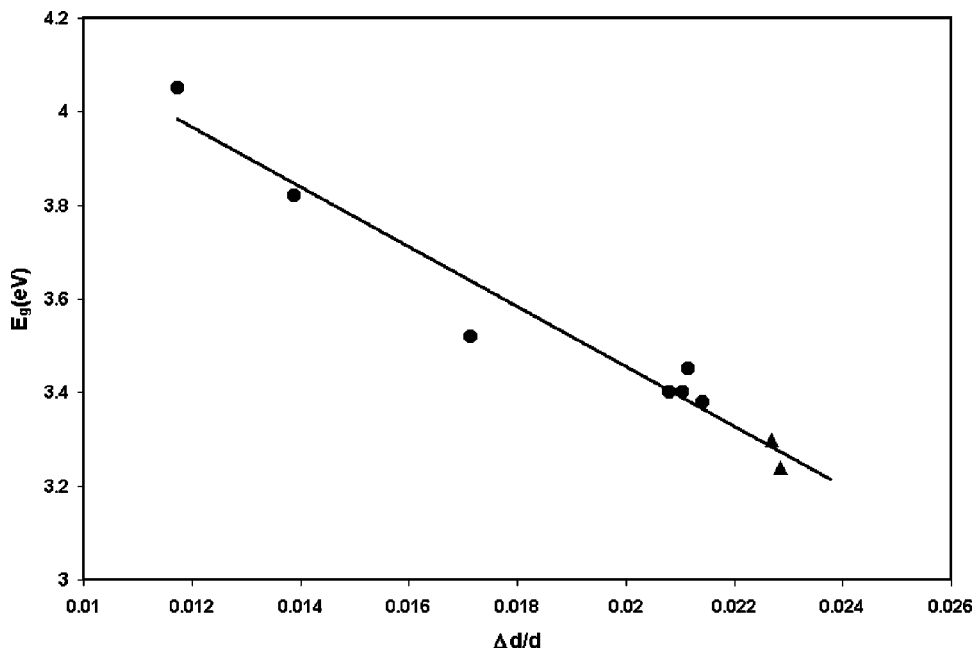


FIG. 7. Dependence of optical band gap on the residual stress in the film for ZnI₂ films. Data points shown by filled triangles were obtained by heat-treatment experiment carried out on a grown 470-nm-thick film.

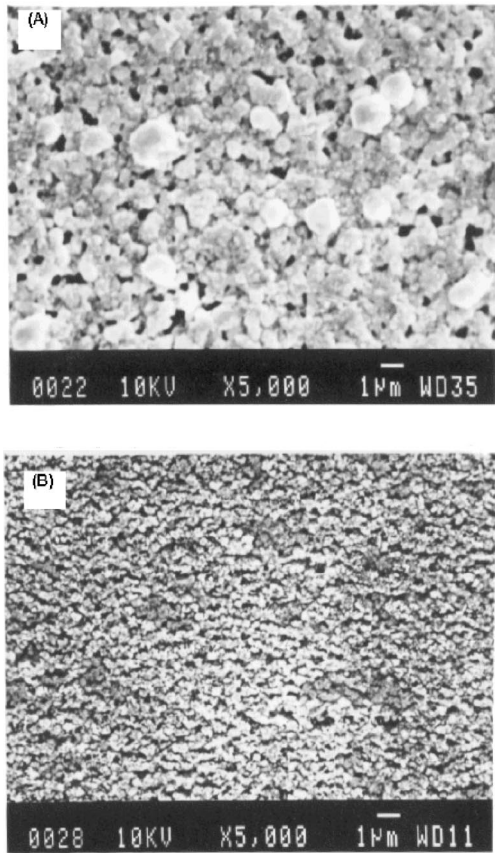


FIG. 8. SEM photographs showing the morphological change from (A) as grown 470-nm-thick ZnI_2 films to that of (B) heat treated (for 30–40 s) at 100 °C in air.

eters in Table I as reported in the literature. It is quite hard to correlate the structural and optical properties of all three compounds together due to their slightly different atomic arrangements in the unit cell.

The magnitude of the band gap determined by extrapolation from Fig. 5 was found to be film thickness dependent as shown in Fig. 6. This type of behavior may indicate quantum size effect. However, even the minimum film thickness in the present study is too large to observe quantum size effect. Therefore, the variation of E_g with film thickness certainly cannot be attributed to quantum size effect. The variation in energy gap with externally applied pressure (stress) is well known. However, even the internal residual stress in the film due to random orientation of crystallites should also affect the band gap. Therefore, we plot E_g vs $\Delta d/d$ in Fig. 7 to examine such a correlation. We can see a linear relationship between them in the limited region of observations. Further, we have tried to confirm the residual-stress-induced band-gap change by another experiment in which a 470-nm-thick film was heat-treated in air for very short duration (30–40 s) at two different temperatures, 100 °C and 150 °C. All the analyses were carried out on these samples. The result of this experiment is shown in Fig. 7 by a separate symbol (filled triangles). The data points obtained in this experiment fits well the linear relationship between E_g and $\Delta d/d$. We can

see that the residual stress increased with heat treatment inducing a proportional reduction in E_g . Again, as mentioned earlier the increase in residual stress resulted from the increased packing density and size distribution of crystallites as can be seen by SEM in Fig. 8. Therefore, the results of heat-treatment experiment strongly supports the results of thickness dependence. Both a decrease and an increase in E_g with $\Delta d/d$ in (002) and (102) oriented films of HgI_2 was observed earlier⁵ due to the anisotropic nature of E_g . There is no report regarding stress (either internal or external)-induced change in optical properties of CdI_2 . We are working on it and a decrease of E_g above certain threshold $\Delta d/d$ has been observed. The results and detailed analysis will be published soon. The intercept of linear fit of Fig. 7 gives the band-gap value of 4.75 eV for a stress-free perfect crystal. A large decrease of band gap with residual stress can be seen from the figure. The slope gives the magnitude of the decrease as $-65 \text{ eV}/(\Delta d/d)$. The large decrease in the band-gap can be realized due to the modification of energy band structure caused by the compression of the unit cell. We can see a large c/a (2.72) for ZnI_2 meaning lot of empty space between layers. Therefore, even the small compressional strain could produce quite appreciable change in band structure. However, there is not much information available regarding ZnI_2 in the literature for the purpose of comparison or estimation. Therefore, we strongly believe that the present paper about ZnI_2 could be quite useful for further investigations to understand the layer compounds better, especially the group *Ib* iodides.

IV. CONCLUSIONS

The optical-absorption measurements carried out at room temperature on structurally, compositionally, and morphologically well-characterized ZnI_2 films reveal an excitonic absorption peak at 3.5 eV with binding energy of 660 meV and a direct-type band gap. The band gap shows thickness dependence that correlates well with the compressive residual stress behavior with film thickness. The thickness dependence of residual stress is attributed to the thickness dependence of packing density and size distribution of crystallite grains observed by morphological analysis. A large decrease in band gap with residual stress is attributed to the large c/a . The linear dependence of E_g with residual stress yields a band-gap value of 4.75 eV for a stress-free perfect crystal.

ACKNOWLEDGMENTS

We would like to thank Dr. P. Arun, Vinod Kumar Paliwal, Ashutosh Bhardwaj, Rajni, Rajeevi, and Hina for their helpful discussions and Mr. P.C. Padmakshan, Department of Geology, University of Delhi, for carrying out x-ray diffraction measurements. The help of Dr. N.C. Mehra, USIC, Delhi University, in the measurements of EDAX and SEM was gratefully acknowledged.

*Email address: agni@physics.du.ac.in

- ¹F. Hullinger, *Structural chemistry of layer type phases* (Reidel, Publishing Co., Dordrecht, Holland, 1976).
- ²P.P.H. Fourcry, D. Carre, and J. Rivet, *Acta Crystallogr., Sect. B: Struct. Crystallogr. Cryst. Chem.* **B34**, 3160 (1978).
- ³K. Hilpert, L. Bencivenni, and B. Saha, *J. Chem. Phys.* **83**, 5227 (1985).
- ⁴P. Tyagi, A.G. Vedeshwar, and N.C. Mehra, *Physica B* **304**, 166 (2001), and references therein.
- ⁵P. Tyagi and A.G. Vedeshwar, *Phys. Rev. B* **63**, 245315 (2001), and references therein.
- ⁶*Crystal Data Determinative Tables, Inorganic Compounds*, 3rd ed., edited by J.D.H. Donnay and H.M. Ondik (Joint Committee on Powder Diffraction Standards, Swarthmore, 1973).
- ⁷B.D. Cullity, *Elements of X-ray diffraction*, 2nd ed. (Addison-Wesley Reading, 1978), p. 286.
- ⁸L.I. Maissel and R. Glang, *Handbook of Thin Film Technology* (McGraw-Hill, New York, 1970).
- ⁹A.E. Ennos, *Appl. Opt.* **5**, 51 (1966).
- ¹⁰C. Kittel, *Introduction to Solid State Physics*, 5th ed. (Wiley Eastern Limited, New Delhi, 1984), p. 333.
- ¹¹P.Y. Yu and M. Cardona, *Fundamentals of Semiconductors*, 2nd ed. (Springer-Verlag, Berlin, 1999), pp. 258–266.
- ¹²D.L. Greenaway and R. Nitsche, *J. Phys. Chem. Solids* **26**, 1445 (1965).
- ¹³R. Coehoorn, G.A. Sawatzky, C. Haas, and R.A. deGroot, *Phys. Rev. B* **31**, 6739 (1985).
- ¹⁴D.E. Turner and B.N. Harmon, *Phys. Rev. B* **40**, 10 516 (1989).
- ¹⁵H. Yao, B. Johs, and R.B. James, *Phys. Rev. B* **56**, 9414 (1997).
- ¹⁶R.H. Bube, *Phys. Rev.* **106**, 703 (1957).